

---

# Fermionic boundary conditions and the finite temperature transition of QCD

Erek Bilgici<sup>a</sup>, Falk Bruckmann<sup>b,c</sup>, Julia Danzer<sup>a</sup>, Christof Gattringer<sup>a</sup>,  
Christian Hagen<sup>c</sup>, Ernst Michael Ilgenfritz<sup>d</sup>, Axel Maas<sup>a</sup>

<sup>a</sup>Institut f. Physik, Universität Graz, 8010 Graz, Austria

<sup>b</sup>Institut f. Theoretische Physik III, Universität Erlangen, 91058 Erlangen, Germany

<sup>c</sup>Institut f. Theoretische Physik, Universität Regensburg, 93040 Regensburg, Germany

<sup>d</sup>Institut f. Theoretische Physik, Universität Heidelberg, 69120 Heidelberg, Germany

## Abstract

Finite temperature lattice QCD is probed by varying the temporal boundary conditions of the fermions. We develop the emerging physical behavior in a study of the quenched case and subsequently present first results for a fully dynamical calculation comparing ensembles below and above the phase transition. We show that for low temperature spectral quantities of the Dirac operator are insensitive to boundary conditions, while in the deconfined phase a non-trivial response to a variation of the boundary conditions sets in.<sup>1</sup>

## 1 Introduction

Understanding the nature and mechanisms of the QCD phase transition has recently become one of the great issues of non-perturbative QCD studies. Questions such as "How can one characterize the high temperature plasma phase?", or "What are the field excitations that drive the transition?", are still far from having a generally accepted answer. A powerful approach to analyzing such questions is the formulation of QCD on a Euclidean space time lattice. In this setting Monte Carlo simulations allow one to obtain non-perturbative results from an ab-initio calculation.

In the Euclidean formulation one dimension, the Euclidean time, is compactified, turning the base manifold into a (hyper) cylinder. The circumference of the cylinder is the inverse temperature. Thus increasing the temperature means shrinking the temporal extent of the lattice. If the temperature is sufficiently high, the temporal extent is shorter than the relevant scale  $\Lambda_{QCD}$ , and correlations around the compact time direction change the physics. The onset of such a strong self-correlation around time corresponds to the critical transition temperature  $T_c$ .

---

<sup>1</sup> Contribution prepared for a special issue of *Few Body Systems* on the occasion of Willibald Plessas' sixtieth birthday. Happy birthday Willi !

This qualitative insight about the relation of the scale  $\Lambda_{QCD}$  and the time extent given by the inverse temperature can be tested on the lattice. A powerful approach to such an analysis is the use of the temporal boundary conditions as a tool. Instead of using the canonical choice – periodic boundary conditions for the gauge fields and anti-periodic boundary conditions for the fermions – one may implement more general temporal boundary conditions to probe the system. According to the qualitative picture outlined above, one is inclined to expect that below  $T_c$  the system remains relatively unchanged under varying boundary conditions, while above  $T_c$  the response of the system to a change of the boundary conditions should be strong.

In a series of papers the strategy of probing finite temperature QCD with the help of boundary conditions has been explored in quenched calculations. In particular generalized fermion boundary conditions have been considered. Various spectral quantities of the Dirac operator were studied [1,2,3,4,5,6,7]. A new observable was proposed and studied [8,9,10,11], the dual chiral condensate, which probes the dependence on the boundary conditions and provides a link between the Polyakov loop and the conventional chiral condensate.

The analysis was also extended beyond the gauge group SU(3). Quenched studies for the center-trivial group  $G_2$  [12] and for SU(2) gauge theory with adjoint fermions [13] were conducted.

In all these quenched studies it was established, that below  $T_c$  the Dirac spectrum is insensitive to the temporal fermion boundary conditions. Above the deconfinement transition, which in the quenched case is characterized by the emergence of a non-vanishing expectation value of the Polyakov loop, a non-trivial response to changing temporal boundary conditions sets in for fermionic quantities such as the chiral condensate and the spectral gap. It was furthermore observed [1,8,9,10,14,15] that only the relative phase between the phase of the Polyakov loop and the phase in the fermionic boundary condition is relevant for the physics. This even holds for the center-trivial group  $G_2$ , which behaves similar to SU(N) when one restricts the high temperature ensembles to the center sector characterized by a real Polyakov loop.

Interesting is also the case of SU(2) (more generally SU(N)) with adjoint fermions [13], a theory where the deconfinement and chiral symmetry restoration temperatures do not coincide, the latter being considerably higher than the former. In agreement with the picture outlined above, at the deconfinement temperature the spectrum becomes sensitive to the boundary conditions. The intermediate phase between the deconfinement and chiral restoration temperatures is characterized by a non-vanishing density of eigenvalues near the origin, and thus, due to the Banks-Casher relation [16] by a non-vanishing chiral condensate, which, however, varies in size with the boundary condition. Only above the chiral restoration temperature the condensate vanishes completely for the physical anti-periodic fermion boundary conditions.

In the first part of this contribution, in Section 2, we discuss the physical situation for the interplay of boundary conditions and spectral observables for the quenched case. In the second part, in Section 3, we present first preliminary results for lattice QCD with dynamical fermions. In particular we analyze publicly available dynamical SU(3) configurations generated for two flavors of staggered sea quarks by the MILC collaboration [17]. Ensembles below and above the QCD transition are studied with the staggered Dirac operator and we compare the response of various spectral quantities below and above  $T_c$  to changing boundary conditions. In Section 4 we summarize our results and give an outlook.

## 2 The physical situation for the quenched case

As outlined in the introduction, the interplay of fermionic boundary conditions and the spectral quantities of the Dirac operator below and above  $T_c$  so far was analyzed only for the quenched case. Although by neglecting the dynamical quark effects the quenched case certainly does not reflect the full problem, as a toy model it has one important conceptual advantage: It represents the passive response of the (fermionic) observables for a sudden (smooth for  $SU(2)$ ) transition of the gluonic environment. For  $SU(N)$ ,  $N > 2$ , there is a first order transition between the two phases and one can expect to find a distinctly different behavior of the Dirac operator below and above  $T_c$ . The fully dynamical theory, on the other hand, shows only a crossover, thus leading to a gradual variation of the properties rather than a sharp change. For that reason the quenched case is an interesting model laboratory.

The calculations were done on  $SU(3)$  gauge ensembles with 100 configurations each, generated with the Lüscher Weisz gauge action [18] with tadpole improvement. When we quote results in physical units, these were obtained from a determination of the scale [19] using the Sommer parameter. Our fermionic observables were computed for the staggered Dirac operator (we here set the lattice spacing to  $a = 1$ )

$$D(x, y) = \sum_{\mu} \eta_{\mu}(x) \left[ U_{\mu}(x) \delta_{x+\hat{\mu}, y} - U_{\mu}(x - \hat{\mu})^{\dagger} \delta_{x-\hat{\mu}, y} \right], \quad (1)$$

where  $\eta_{\mu}(x)$  is the staggered sign function  $\eta_{\mu}(x) = \prod_{\nu=1}^{\mu-1} (-1)^{x_{\nu}}$ . For the massless staggered lattice Dirac operator (1) we evaluate complete eigenvalue spectra using a parallel implementation of standard linear algebra routines. The staggered Dirac operator is anti-hermitian and consequently the eigenvalues  $\lambda^{(j)}$  are purely imaginary. The eigenvalues for the Dirac operator with mass  $m$  are then given by  $\lambda^{(j)} + m$ . From the complete eigenvalue spectra all our fermionic observables may be computed.

As outlined in the introduction, we probe the system by changing the temporal fermionic boundary conditions. These are introduced as,

$$\psi(\mathbf{x}, N_T) = e^{i\phi} \psi(\mathbf{x}, 0), \quad (2)$$

where  $N_T$  is the number of lattice points in the compact time direction and the "boundary angle"  $\phi \in [0, 2\pi]$  parameterizes the boundary conditions. Bilinear combinations (which are bosons) are periodic. A value of  $\phi = \pi$  corresponds to the usual anti-periodic boundary conditions. Other values are adopted to analyze the system. In particular we consider a total of eight (for some tests also 16 up to 128) equally spaced intermediate values of  $\phi$  in the interval  $[0, 2\pi]$ . For completeness we stress, that all other boundary conditions, i.e., the spatial fermionic boundary conditions and the boundary conditions for the gauge fields, were kept periodic. We work with various lattice sizes ranging from  $8^3 \times 4$  to  $14^3 \times 6$ , with typically 100 configurations per ensemble. All errors we show are statistical errors determined with single elimination Jackknife.

Let us begin the discussion of observables with the bare (unrenormalized) chiral condensate. In terms of the eigenvalues it is given by

$$-\langle \bar{\psi} \psi \rangle = \lim_{m \rightarrow 0} \lim_{V \rightarrow \infty} \frac{1}{V} \text{Tr} (D + m)^{-1} = \lim_{m \rightarrow 0} \lim_{V \rightarrow \infty} \frac{1}{V} \sum_j \frac{1}{\lambda^{(j)} + m}, \quad (3)$$

where  $V$  is the 4-volume and  $m$  the quark mass parameter. Obviously it is not possible to perform the thermodynamic limit on a finite lattice. Two alternative approaches

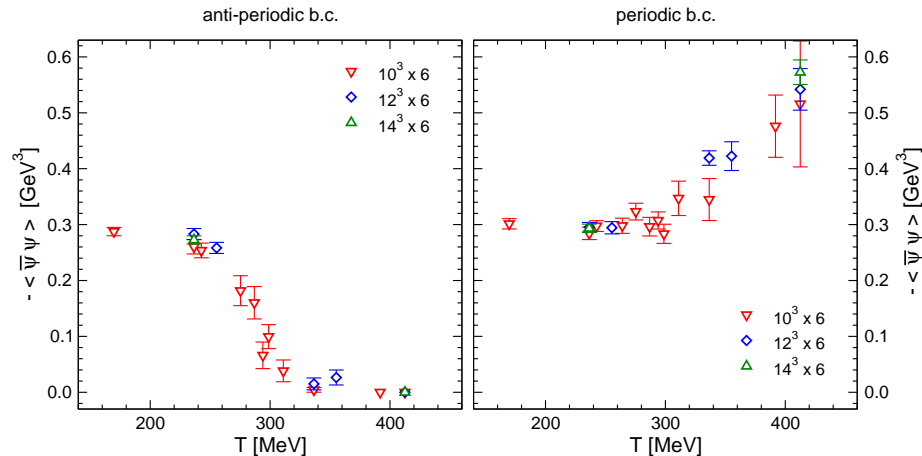


**Fig. 1** The bare quenched chiral condensate  $-\langle\bar{\psi}\psi\rangle$  in  $\text{GeV}^3$  for anti-periodic (lhs. plot) and periodic (rhs.) temporal fermion boundary conditions as a function of temperature.

are possible: Firstly, one may analyze the condensate for finite volume as a function of the mass parameter  $m$  and extrapolate to  $m = 0$ , ignoring the sharp drop to 0 at  $m = 0$ , which must appear as long as the volume is finite. Secondly, one can use the Banks-Casher formula [16], which relates the chiral condensate to the spectral density  $\rho(0)$  at the origin,

$$-\langle\bar{\psi}\psi\rangle = \pi\rho(0), \quad (4)$$

and determine  $\rho(0)$  to compute the chiral condensate. It can be shown [12] that for a fixed volume both methods give rise to perfectly consistent results.

In Fig. 1 we show the bare chiral condensate  $-\langle\bar{\psi}\psi\rangle$  as a function of the temperature. In the lhs. plot we display the results for the physical anti-periodic temporal fermion boundary conditions, while the rhs. plot is for periodic boundary conditions. It is obvious, that the two cases behave rather differently. For the physical anti-periodic boundary conditions the condensate starts to melt near the critical temperature of  $T_c \simeq 280$  MeV, while for the periodic case the bare condensate even rises beyond  $T_c$ . Below the critical temperature the anti-periodic and the periodic data essentially agree, thus reinforcing the expectation that below  $T_c$  the system is insensitive to the imposed boundary conditions, while above  $T_c$  (many) physical quantities show a non-trivial dependence on the boundary conditions.

According to the Banks-Casher relation [16] a vanishing condensate, as we observe it for the anti-periodic boundary conditions at high temperatures, must coincide with a vanishing spectral density  $\rho(0)$ . Such a vanishing density above  $T_c$  is usually attributed to the opening up of a gap in the spectrum. We analyze the spectral gap using the expectation value  $\langle|\lambda_{min}|\rangle$ , where  $\lambda_{min}$  is the smallest eigenvalue of the Dirac operator.

In Fig. 2 we show the results for the spectral gap as a function of the temperature, where we again compare the physical anti-periodic boundary conditions (lhs.) to the periodic case (rhs.). As for the condensate, we find also for the spectral gap that up to  $T_c \simeq 280$  MeV the two cases give roughly the same results, while above  $T_c$  we observe a non-trivial response to a change of the boundary conditions. For the anti-periodic boundary conditions, we find that above  $T_c$  the spectral gap opens up quickly

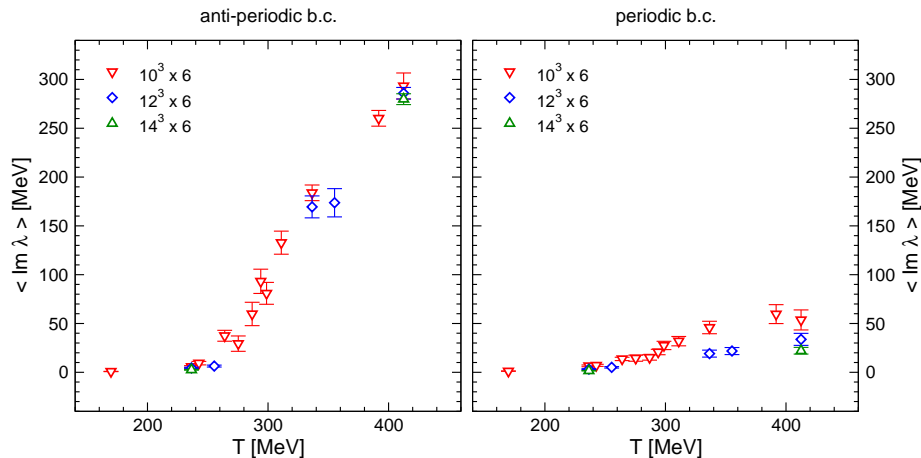


**Fig. 2** The quenched spectral gap in MeV for anti-periodic (lhs. plot) and periodic (rhs.) temporal fermion boundary conditions as a function of temperature.

in accordance with the vanishing condensate for that case demonstrated in the lhs. plot of Fig. 1. When inspecting the periodic case on the rhs. plot of Fig. 2 we do not observe the opening up of a spectral gap. There is a slight upward trend, but way less pronounced than for the anti-periodic boundary conditions. This upward trend for the periodic case also becomes weaker as the spatial volume is increased and thus is probably a finite size effect, similar to the "microscopic gap"  $\propto 1/V_{space}$  known from random matrix theory [20].

Although the picture for the spectral gap seems rather clear, there is an interesting alternative scenario to be considered: The vanishing spectral density at the origin,  $\rho(0)$ , which according to the Banks-Casher formula (4) is necessary for a vanishing chiral condensate, does not necessarily imply a spectral gap. An alternative would be a spectral density that is non-vanishing for all non-zero eigenvalues but continuously goes to zero at the origin. This would imply that the spectral gap of the lattice Dirac operator, shown in the lhs. plot of Fig. 2, closes as the spatial volume is sent to infinity. The currently available data do not allow one to decide between a closing gap at infinite spatial volume or a finite limit for the gap [5, 21].

In this context we also stress that the staggered lattice Dirac operator is numerically cheap, but certainly not the first choice for analyzing the chiral condensate and the spectral gap. The reason is that the staggered Dirac operator does not discriminate between low lying eigenvalues and eigenvalues that correspond to zero modes originating from topological excitations. The latter, however, should be removed in both the determination of the spectral gap, as well as for the evaluation of the spectral density  $\rho(0)$ . Using, e.g., the overlap operator would allow for a cleaner study – at a considerably higher computational cost, however.

We have seen that above  $T_c$  the spectral gap and the chiral condensate, which in turn through (4) is related to the spectral density  $\rho(0)$  at the origin, are sensitive to the fermionic boundary conditions. Both the spectral gap and the density  $\rho(0)$  are infrared properties of the Dirac spectrum. An interesting question is how the other parts of the Dirac spectrum respond to changing boundary conditions. This question was analyzed

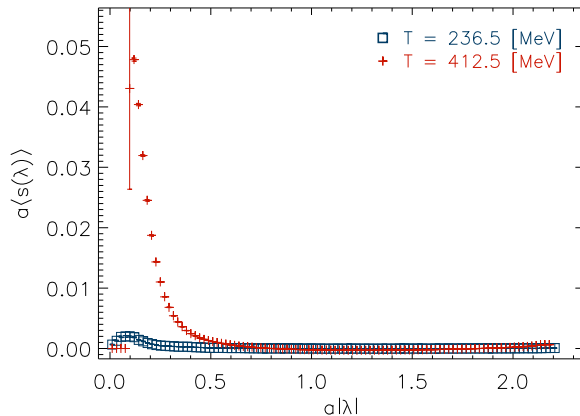


**Fig. 3** The expectation value of the shift variable  $s(\lambda)$  as a function of  $|\lambda|$  (both in lattice units). The data are for the quenched  $14^3 \times 6$  lattices and we compare two ensembles below ( $T = 236.5$  MeV) and above  $T_c$  ( $T = 412.5$  MeV).

numerically in [?,10] and analytically in [4]. It was found that the IR modes of the Dirac spectrum are most sensitive to a change of the boundary conditions, while the shift of the eigenvalues under a variation of the boundary angle  $\phi$  decreases exponentially as one moves towards the UV end of the spectrum.

In order to quantify this shift, in Fig. 3 we show the shift  $s(\lambda)$  of the eigenvalues when comparing boundary conditions with  $\phi = \pi/2$  and boundary conditions with boundary angle  $\phi = \pi$ . More explicitly, the shift variable  $s(\lambda)$  is defined as

$$s(\lambda) = \text{Im} \left( \lambda_{\phi=\pi/2} - \lambda_{\phi=\pi} \right). \quad (5)$$

In Fig. 3 we plot this shift observable as a function of the size of the physical ( $\phi = \pi$ ) eigenvalue (both quantities in lattice units), and compare the results below and above  $T_c$ . It is obvious that in both cases a noticeable shift is seen only for the IR part of the spectrum, and  $s(\lambda)$  decreases quickly towards the UV end of the spectrum. The plot also again confirms that only above  $T_c$  there is a sizable shift of the eigenvalues when changing the boundary conditions. Let us finally comment on the drop of the shift variable at  $\lambda \simeq 0$ : We attribute this effect to the would-be zero modes of the staggered Dirac operator. For a chiral operator such as the overlap operator, they would be frozen at the origin when changing the boundary conditions. The staggered operator does not protect them from a shift, but the nature of the would-be zero modes is at least manifest in a drop of the shift variable  $s(\lambda)$  at  $\lambda \simeq 0$ .

So far we have only compared two values of the boundary angle  $\phi$ . In Fig. 4 we now show how the lowest 40 eigenvalues of the Dirac operator in the quenched case behave as a function of  $\phi$ . It is obvious, that for ensembles below  $T_c$  (top plot) the eigenvalues are essentially independent of  $\phi$ . Above  $T_c$  they show a sine-like behavior as a function of  $\phi$ . For the sector where the Polyakov loop is essentially real (center plot), the lowest eigenvalues come close to zero for the case of periodic boundary conditions ( $\phi = 0$ ). For the case of configurations in a sector with complex Polyakov loop (bottom plot), the displacement pattern of the eigenvalues is shifted by  $\pm 2\pi/3$ .

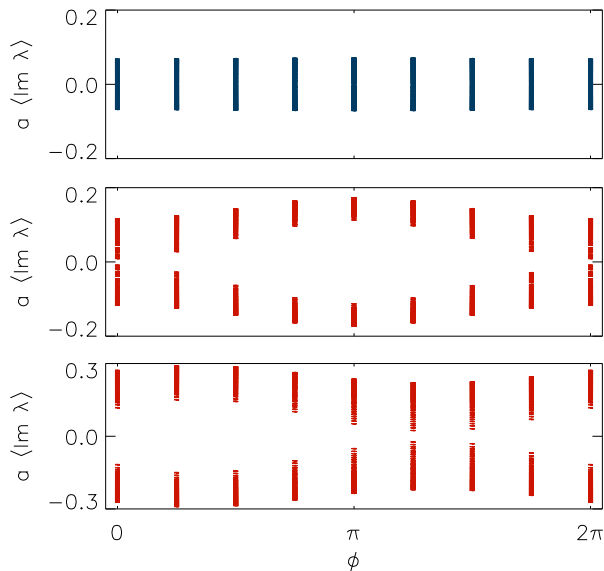


**Fig. 4** We show the lowest 40 eigenvalues of the lattice Dirac operator for various values of the boundary angle  $\phi$  using our  $14^3 \times 6$  quenched ensembles ( $8^3 \times 4$  for the bottom plot). The top plot is for a temperature below  $T_c$ , while the other two plots are for  $T > T_c$ . They differ by the sector of the Polyakov loop: In the center plot we use a configuration in the real Polyakov loop sector, while at the bottom the eigenvalues are shown for the sector where the phase of the Polyakov loop is close to  $2\pi/3$ .

For the quenched case the Polyakov loop is an order parameter for the deconfinement transition [22]. It signals the breaking of the center symmetry, which for the quenched theory is manifest below  $T_c$  and the expectation value of the Polyakov loop is zero then. Above  $T_c$  the center symmetry becomes broken spontaneously and the Polyakov loop acquires a non-vanishing expectation value. Its phase spontaneously selects one of the three (for  $SU(3)$ ) values,  $0, 2\pi/3, -2\pi/3$ .

One of the original motivations [2] for analyzing the connection between boundary conditions and the Dirac spectrum, was to find out, how the change of the Polyakov loop at the phase transition affects properties of spectral sums of Dirac eigenvalues. The Polyakov loop is an order parameter for confinement, while certain spectral sums of the Dirac operator, e.g., the one in Eq. (3), are related to chiral symmetry. Thus understanding the relation between the Polyakov loop and the Dirac spectrum might provide an understanding of a possible relation between chiral symmetry breaking and deconfinement. It is natural to expect that the Dirac operator and its spectral properties connect both, confinement and chiral symmetry. After all, the quark-propagator, i.e., the inverse Dirac operator, should know whether the quark it describes is in the chirally symmetric or the chirally broken phase, and if it is confined or not.

For understanding the relation between the chiral condensate and the Polyakov loop we write the condensate in a rather general form: The chiral condensate is a gauge invariant quantity, and as such may be written as a sum of (traced) gauge transporters

along closed loops on the lattice,

$$-\bar{\psi}\psi = \sum_{l \in \mathcal{L}} c(l) \text{Tr} \prod_{(x,\mu) \in l} U_\mu(x). \quad (6)$$

Here  $\mathcal{L}$  is the set of all loops that contribute,  $l$  is an individual loop in this set,  $c(l)$  a complex valued coefficient, and the product runs over all links in  $l$ . We remark that the structure in Eq. (6) is universal and different lattice discretizations of the lattice Dirac operator only lead to different values for the coefficients  $c(l)$ .

On a finite lattice it is possible to order all loops  $l$  in (6) according to their winding number  $q$  around the compact time direction. If we implement the boundary condition (2), then the loops pick up a phase  $\exp(i\phi)$  with every winding. Thus we can write the condensate for the general boundary condition (2) as

$$-\bar{\psi}\psi \Big|_\phi = \sum_{q \in \mathbb{Z}} e^{i\phi q} \sum_{l \in \mathcal{L}^{(q)}} c(l) \text{Tr} \prod_{(x,\mu) \in l} U_\mu(x), \quad (7)$$

where  $\mathcal{L}^{(q)}$  is the set of all loops that wind exactly  $q$ -times. Using a Fourier transformation with respect to the boundary angle we can project to the contributions that wind exactly once, and in this way define the dual chiral condensate  $\Sigma^{(1)}$ ,

$$\Sigma^{(1)} = - \int_0^{2\pi} \frac{d\phi}{2\pi} \bar{\psi}\psi \Big|_\phi e^{-i\phi} = \sum_{l \in \mathcal{L}^{(1)}} c(l) \text{Tr} \prod_{(x,\mu) \in l} U_\mu(x), \quad (8)$$

where we used  $\int d\phi \exp(i\phi(q-1)) = 2\pi\delta_{q,1}$  in the second step. The dual chiral condensate  $\Sigma^{(1)}$  consists of the loops of the conventional chiral condensate, but restricted to winding number 1. These loops, however, transform under a center transformation in exactly the same way as the Polyakov loop. Consequently,  $\Sigma^{(1)}$  also serves as an order parameter for the breaking of the center symmetry and thus in the quenched case is an order parameter for confinement. We remark that the technique of using a Fourier transformation with respect to the boundary angle has been used in various contexts, in particular for the construction of canonical determinants, i.e., fermion determinants that describe a fixed quark number.

We stress at this point, that we have not performed the limits  $V \rightarrow \infty$  and  $m \rightarrow 0$  in the definition (8) of the dual chiral condensate, but of course these two limits are necessary when one wants to use  $\Sigma^{(1)}$  for the analysis of chiral symmetry. On the other hand, since the weight factors  $c(l)$  in (8) behave for large  $m$  as  $c(l) \propto m^{-|l|}$ , where  $|l|$  is the length of the loop  $l$ , the infinite mass limit reduces the dual condensate  $\Sigma^{(1)}$  to the shortest loops that wind exactly once, i.e., the conventional straight Polyakov loops.

For a practical evaluation of the dual condensate, we make use of the spectral representation (3) and obtain

$$\Sigma^{(1)} = \int_0^{2\pi} \frac{d\phi}{2\pi} S(\phi) e^{-i\phi}, \quad \text{with} \quad S(\phi) = \frac{1}{V} \sum_j \frac{1}{\lambda_\phi^{(j)} + m}, \quad (9)$$

where  $\lambda_\phi^{(j)}$  denotes the  $j$ -th eigenvalue computed for boundary angle  $\phi$ . The  $\phi$ -integral is evaluated numerically using the eight intermediate values of  $\phi$  in the interval  $[0, 2\pi]$ .

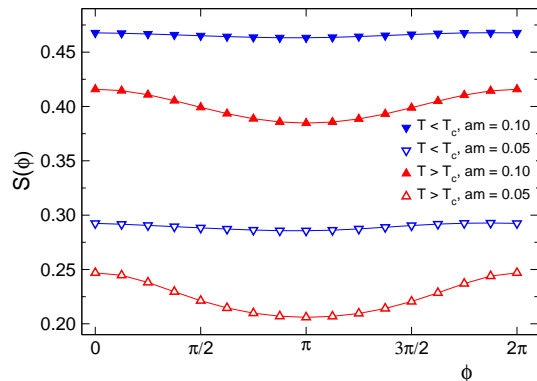


**Fig. 5** The integrand  $S(\phi)$  of the dual chiral condensate in the quenched case as a function of the boundary angle  $\phi$ . We show the results for two bare quark masses and compare ensembles below and above  $T_c$  (Figure from [8].).

Increasing the number of intermediate values further leads only to corrections smaller than one percent.

The dual chiral condensate (9) is the first Fourier component of the spectral sum  $S(\phi)$ . For small quark mass  $m$  this spectral sum is obviously dominated by the IR end of the spectrum and thus should show a non-trivial dependence on  $\phi$  above  $T_c$ , where the IR eigenvalues move when changing boundary condition. Below  $T_c$  the eigenvalues are essentially independent of  $\phi$  and thus  $S(\phi)$  is approximately constant, and (9) implies a vanishing dual chiral condensate below  $T_c$ . This behavior of the spectral sum  $S(\phi)$  is obvious from Fig. 5, where we show  $S(\phi)$  as a function of  $\phi$  at two different bare quark masses  $m$  for two ensembles below and above  $T_c$ .

Finally in Fig. 6 we present the (unrenormalized) dual chiral condensate  $\Sigma^{(1)}$  as a function of the temperature  $T$ . We show results for different lattice volumes and lattice spacings. The bare quark mass was chosen to be  $m = 100$  MeV for all these ensembles. Obviously the dual chiral condensate vanishes below  $T_c \simeq 280$  MeV, while above the transition it acquires a non-vanishing value which rises quickly with  $T$ . It is remarkable that the data points from the rather different ensembles fall essentially on a universal curve, which cannot a-priori be expected for an unrenormalized quantity (the conventional thin Polyakov loop is a counterexample). This hints at simple renormalization properties of the dual chiral condensate.

### 3 Results for QCD with dynamical fermions

We now come to discussing the results for QCD with dynamical fermions. Several aspects change when turning on the sea quarks. There is no longer a sharp transition, but a continuous crossover. Consequently we can expect only a gradually changing behavior of the system. Also the center symmetry is broken explicitly by the fermion determinant. Thus the Polyakov loop and also the dual chiral condensate have a non-vanishing expectation value at low temperatures, which predominantly comes from contributions of the sector with quark number  $q = -1$ .

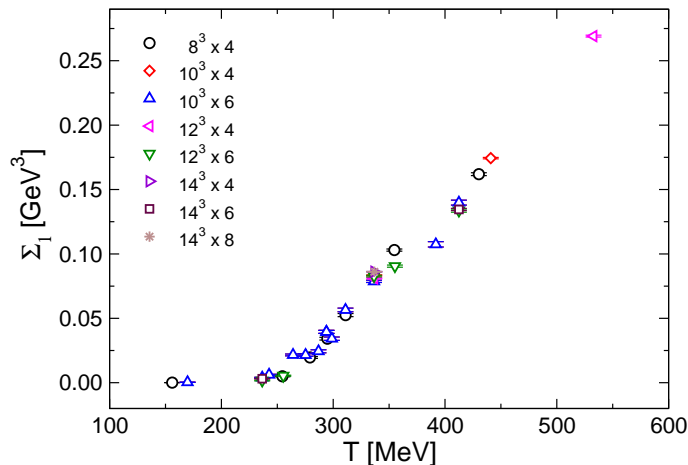


**Fig. 6** The quenched dual chiral condensate in physical units as a function of the temperature (Figure from [8]).

Although several aspects are different for the dynamical case, one can ask the question how much of the physical properties which we discussed for the quenched case are manifest also in the full theory. We will show, that indeed the qualitative behavior is unchanged, with a small sensitivity to the temporal fermion boundary conditions at low temperatures, and a strong response to a variation of the boundary angle  $\phi$  in the high temperature regime.

The dynamical configurations we analyze are from the publicly available ensembles for two flavors of staggered fermions, provided by the "Gauge Connection" [17]. In particular we consider the  $12^3 \times 4$  lattices, and focus on the configurations generated with a bare quark mass of  $m = 0.008$  in lattice units. They are available for six temperature values in a small band near  $T_c \simeq 153$  MeV, with temperatures  $T = 149.8, 151.5, 153.2, 155.0, 156.8$  and  $160.4$  MeV, according to the scale determined in [24]. The generation of these configurations was done with the canonical anti-periodic temporal boundary conditions for the fermions.

We begin the discussion of the dynamical case with showing in Fig. 7 the bare chiral condensate as a function of the boundary angle  $\phi$ . It is obvious, that for the two lowest temperatures there is only a small variation with  $\phi$ , while for the larger values of  $T$  a much stronger response to changing boundary conditions has developed.

In Fig. 8 we study the variation of the 40 lowest eigenvalues with the boundary angle  $\phi$ . We compare the situation in the low temperature phase ( $T = 149.8$  MeV, top plot) and above  $T_c$  ( $T = 160.4$  MeV, bottom). A comparison with the quenched case in Fig. 2 shows that the situation is very similar here: Below  $T_c$  the spectrum is almost independent of  $\phi$ , while above  $T_c$  the sine-like variation is observed. We stress again, that for the unquenched case the Polyakov loop is real, since the fermion determinant is much larger for that Polyakov loop sector (see, e.g., [23]). Thus the shifted scenario depicted in the bottom plot of Fig. 4 is absent for the dynamical case. In this respect the dynamical case is very similar to the behavior of pure  $G_2$  lattice gauge theory [12], where the triviality of the center also allows only for a sector with real Polyakov loop.

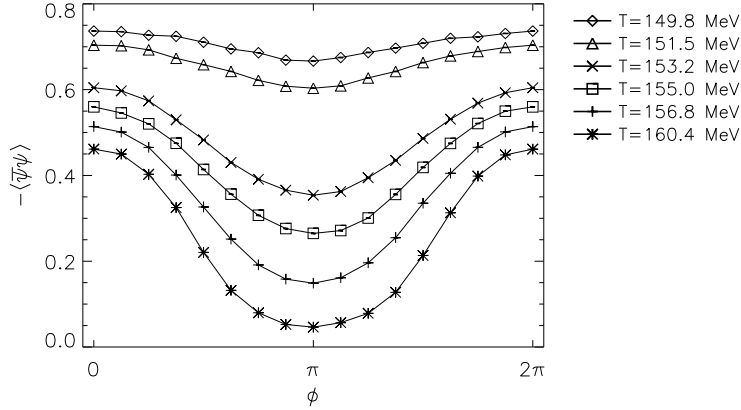


**Fig. 7** The bare chiral condensate of the dynamical theory as a function of the boundary angle  $\phi$  for various temperatures.

The behavior of the IR part of the spectrum shown in Fig. 8 is inherited by the integrand  $S(\phi)$  defined in (9). In Fig. 9 we show  $S(\phi)$  as a function of the boundary angle  $\phi$  and again compare the situations in the low temperature phase ( $T = 149.8$  MeV) and above  $T_c$  ( $T = 160.4$  MeV). The quark mass  $m$  in the definition (9) of the integrand  $S(\phi)$  was set to the sea quark mass  $m = 0.008$  (in lattice units). It is obvious from Fig. 9 that the integrand below  $T_c$  is rather insensitive to the boundary angle, while in the high temperature phase we observe a strong variation with  $\phi$ , which in turn gives a larger value for the dual chiral condensate.

In Fig. 10, we finally show the dual chiral condensate  $\Sigma^{(1)}$  (without any renormalization) as a function of the temperature. Again the quark mass  $m$  in the definition (9) of  $\Sigma^{(1)}$  was set to the sea quark value  $m = 0.008$  (in lattice units). The plot shows clearly that below  $T_c$  the dual chiral condensate is small but non-vanishing, and above

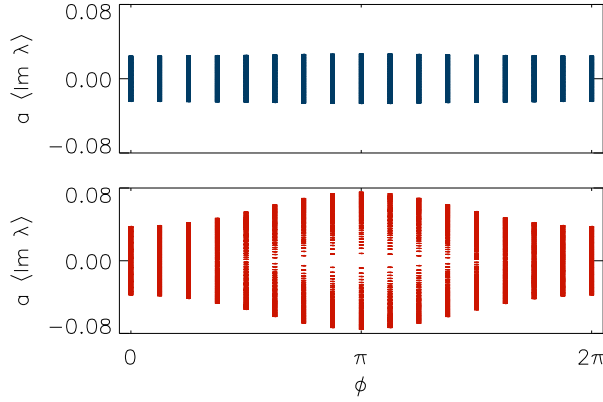


**Fig. 8** The 40 lowest eigenvalues in lattice units at low ( $T = 149.8$  MeV, top plot) and high ( $T = 160.4$  MeV, bottom) temperatures as a function of the boundary angle  $\phi$ .

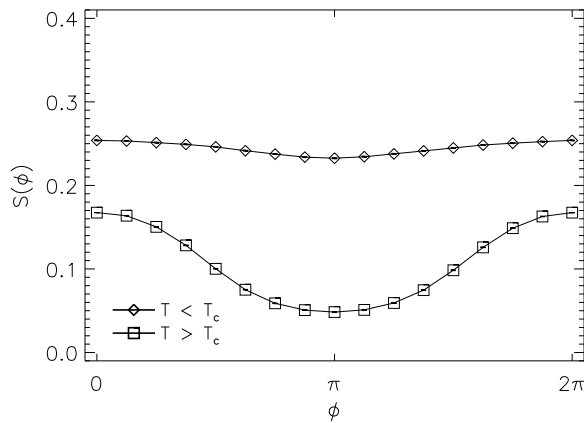


**Fig. 9** The integrand  $S(\phi)$  of the chiral condensate for the dynamical case below and above  $T_c$  as a function of the boundary angle  $\phi$ .

$T_c$  rises quickly with  $T$ . The observable underlines the physical picture of a strongly increased sensitivity to boundary conditions above  $T_c$ .

It is obvious, that the dynamical results presented here have still a preliminary character. In particular the temperatures available to us through the MILC ensembles come from a rather narrow range around  $T_c$ . It would be interesting how quickly the sensitivity to changing boundary conditions goes away for temperatures deeper in the low temperature phase. Also a study with a chiral lattice action for the fermions, e.g., the overlap operator would be desirable, since this would allow one to cleanly remove the contributions of the zero modes.

#### 4 Summary, discussion and outlook

In this contribution we have analyzed the interplay of fermionic temporal boundary conditions and spectral quantities of the Dirac operator for finite temperature lattice QCD. The temporal boundary conditions are used as a tool to probe the system. The underlying working hypothesis is that for low temperature, where the temporal extent of the lattice is large – larger than the scale  $\Lambda_{QCD}$  of the system – the spectral quantities (and also other observables) are essentially insensitive to a change of the boundary conditions. As the temperature  $T$  is increased, the temporal extent of the lattice shrinks, and near  $T_c$  becomes smaller than  $\Lambda_{QCD}$ , and a non-trivial response to changing boundary conditions sets in. In particular the following qualitative features were demonstrated:

- For low temperature the chiral condensate is essentially independent of the boundary conditions. At high temperature it varies with the boundary angle  $\phi$ , and has a minimum for anti-periodic boundary conditions, i.e.,  $\phi = \pi$ . This observation holds for the dynamical case as well as for quenched configurations in the real Polyakov loop sector. For the quenched case with configurations in the complex Polyakov loop sectors the  $\phi$  dependence is shifted by  $\pm 2\pi/3$ .

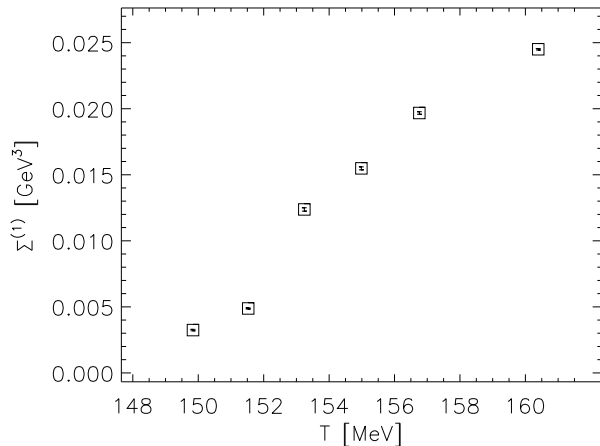


**Fig. 10** The bare dual chiral condensate  $\Sigma^{(1)}$  for the dynamical case as a function of the temperature.

- For low temperatures the spectrum of the Dirac operator is insensitive to changing boundary conditions, while above  $T_c$  the IR modes show a sine-like dependence on the boundary angle  $\phi$ . For the quenched case, again the variation pattern with  $\phi$  is shifted by  $\pm 2\pi/3$  when ensembles for the complex Polyakov loop sectors are considered. The sensitivity of the eigenvalues to changing boundary conditions decreases quickly as one moves towards the UV end of the spectrum.
- The dual chiral condensate is defined as the first Fourier component of the conventional chiral condensate with respect to the boundary angle  $\phi$ , and thus is an observable testing the sensitivity to the boundary conditions. Furthermore, under center rotations (flips) it transforms like the Polyakov loop and thus is also an order parameter for center symmetry. In the quenched case it is zero below  $T_c$  and non-vanishing above  $T_c$ . For the fully dynamical case it is essentially real and positive, with a small but non-vanishing value below  $T_c$ , and a quickly increasing value above the transition.

We stress again that the results for the dynamical case still have a preliminary character (see the last paragraph of Section 3). However, the fact that also for the full theory the finite temperature transition goes along with a strong increase of the sensitivity to temporal fermionic boundary conditions is certainly established.

At this place one may speculate what excitations of the gluon field could drive the effects observed in the fermionic spectra. Dyons (see, e.g., [25]) are natural candidates as their index theorem [26] is sensitive to the boundary conditions: For dyons of given electric and magnetic charge the zero modes exist only in a certain range of boundary angles. These zero modes then mix and form a near-zero mode band. Dyons can be combined into calorons [27,28], which are neutral and always possess zero modes, the latter then hop between the constituent dyons [29].

In a dyon gas model the different dyons appear independently according to their masses, which in turn are governed by the holonomy. For a holonomy corresponding to the confined phase all dyons are equally abundant and changing the boundary condi-

tions will therefore not affect the number of zero modes. For a holonomy corresponding to the deconfined phase, however, some dyons become heavier than others and the abundance of zero modes depends on the boundary angle. For  $SU(2)$  the relation to the angle of the Polyakov loop is just as described above [15]. This suppression effect has been investigated on the lattice [30] and might also explain the decrease of the topological susceptibility above  $T_c$  [31]. These ideas certainly should be substantiated further with lattice methods – a task which we leave for future studies.

Another interesting and important challenge is to analyze the role of temporal boundary conditions as a tool for probing finite temperature QCD using non-lattice methods. Only very little has been attempted in this direction so far [4,11]. Understanding better the response of the system to changing boundary conditions certainly will help to characterize the phases of QCD and the mechanisms driving the transition.

**Acknowledgements** The authors thank Christian Fischer, Tamas Kovacs, Christian Lang, Boris Martemyanov, Michael Müller-Preussker, Maria Paola Lombardo, Jan Pawłowski and Andreas Wipf for discussions. This work is partly supported by the Fonds zur Förderung der Wissenschaftlichen Forschung under grants DK W1203-N08, M1099-N16 and P20330, by the DFG under grant number BR 2872/4-1, and the European Union FP7 program "Hadron Physics 2" grant number 227431. The simulations were done on the clusters of the ZID, University of Graz.

## References

1. C. Gattringer and S. Schaefer, Nucl. Phys. B **654** (2003) 30 [arXiv:hep-lat/0212029].
2. C. Gattringer, Phys. Rev. Lett. **97** (2006) 032003 [arXiv:hep-lat/0605018]; F. Bruckmann, C. Gattringer and C. Hagen, Phys. Lett. B **647** (2007) 56 [arXiv:hep-lat/0612020]; C. Hagen, F. Bruckmann, E. Bilgici and C. Gattringer, PoS **LAT2007** (2007) 289 [arXiv:0710.0294 [hep-lat]].
3. F. Synatschke, A. Wipf and C. Wozar, Phys. Rev. D **75** (2007) 114003 [arXiv:hep-lat/0703018].
4. F. Synatschke, A. Wipf and K. Langfeld, Phys. Rev. D **77** (2008) 114018 [arXiv:0803.0271 [hep-lat]].
5. T. G. Kovacs, PoS **LATTICE2008** (2008) 198 [arXiv:0810.4763 [hep-lat]].
6. E. Bilgici and C. Gattringer, JHEP **0805** (2008) 030 [arXiv:0803.1127 [hep-lat]].
7. W. Söldner, PoS **LAT2007** (2007) 222 [arXiv:0710.2707 [hep-lat]].
8. E. Bilgici, F. Bruckmann, C. Gattringer and C. Hagen, Phys. Rev. D **77** (2008) 094007 [arXiv:0801.4051 [hep-lat]].
9. F. Bruckmann, C. Hagen, E. Bilgici and C. Gattringer, PoS **LATTICE2008** (2008) 262 [arXiv:0810.0899 [hep-lat]].
10. E. Bilgici, *Signatures of confinement and chiral symmetry breaking in spectral quantities of lattice Dirac operators*, PhD Thesis, University of Graz, Austria, 2009 (<http://physik.uni-graz.at/itp/files/bilgici/dissertation.pdf>).
11. C. S. Fischer, arXiv:0904.2700 [hep-ph].
12. J. Danzer, C. Gattringer and A. Maas, JHEP **0901** (2009) 024 [arXiv:0810.3973 [hep-lat]].
13. E. Bilgici, C. Gattringer, E. M. Ilgenfritz and A. Maas, arXiv:0904.3450 [hep-lat].
14. C. Gattringer, P. E. L. Rakow, A. Schäfer and W. Söldner, Phys. Rev. D **66** (2002) 054502 [arXiv:hep-lat/0202009].
15. V. G. Bornyakov, E. V. Luschevskaya, S. M. Morozov, M. I. Polikarpov, E. M. Ilgenfritz and M. Müller-Preussker, Phys. Rev. D **79** (2009) 054505 [arXiv:0807.1980 [hep-lat]].
16. T. Banks and A. Casher, Nucl. Phys. B **169** (1980) 103.
17. MILC collaboration, "The Gauge Connection", ensembles available at <http://qcd.nersc.gov/>
18. M. Lüscher and P. Weisz, Commun. Math. Phys. **97**, 59 (1985); Err.: **98**, 433 (1985); G. Curci, P. Menotti, and G. Paffuti, Phys. Lett. B **130**, 205 (1983); Err.: B **135**, 516 (1984).

- 
19. C. Gatttringer, R. Hoffmann and S. Schaefer, Phys. Rev. D **65** (2002) 094503 [arXiv:hep-lat/0112024].
  20. J. J. M. Verbaarschot and T. Wettig, Ann. Rev. Nucl. Part. Sci. **50** (2000) 343 [arXiv:hep-ph/0003017].
  21. T. Kovacs, private communication.
  22. L. McLerran, B. Svetitsky, Phys. Rev. D **24**, 450 (1981).
  23. C. Gatttringer and L. Liptak, arXiv:0906.1088 [hep-lat].
  24. C. W. Bernard *et al.*, Phys. Rev. D **54** (1996) 4585 [arXiv:hep-lat/9605028].
  25. F. Bruckmann, Eur. Phys. J. ST **152** (2007) 61 [arXiv:0706.2269 [hep-th]]; D. Diakonov, arXiv:0906.2456 [hep-ph].
  26. C. Callias, Commun. Math. Phys. **62** (1978) 213; T. M. W. Nye and M. A. Singer, arXiv:math/0009144.
  27. T. C. Kraan and P. van Baal, Nucl. Phys. B **533** (1998) 627 [arXiv:hep-th/9805168].
  28. K. M. Lee and C. h. Lu, Phys. Rev. D **58** (1998) 025011 [arXiv:hep-th/9802108].
  29. M. Garcia Perez, A. Gonzalez-Arroyo, C. Pena and P. van Baal, Phys. Rev. D **60** (1999) 031901 [arXiv:hep-th/9905016].
  30. V. G. Bornyakov, E. M. Ilgenfritz, B. V. Martemyanov and M. Müller-Preussker, Phys. Rev. D **79** (2009) 034506 [arXiv:0809.2142 [hep-lat]].
  31. F. Bruckmann, arXiv:0901.0987 [hep-ph].